

LIGHT CHARGED PARTICLES AS GATEWAY TO HYPERDEFORMATION*

B. HERSKIND^a, G.B. HAGEMANN^a, TH. DØSSING^a, C. RØNN HANSEN^a
 N. SCHUNCK^{a,u}, G. SLETTEN^a, S. ØDEGÅRD^{a,v}, H. HÜBEL^b, P. BRINGEL^b
 A. BÜRGER^b, A. NEUSSER^b, A.K. SINGH^b, A. AL-KHATIB^b, S.B. PATEL^b,
 B.M. NYAKÓ^c, A. ALGORA^c, Z. DOMBRÁDI^c, J. GÁL^c, G. KALINKA^c, D. SOHLER^c
 J. MOLNÁR^c, J. TIMÁR^c, L. ZOLNAI^c, K. JUHÁSZ^d, A. BRACCO^e, S. LEONI^e
 F. CAMERA^e, G. BENZONI^e, P. MASON^e, A. PALENI^e, B. MILLION^e, O. WIELAND^e
 P. BEDNARCZYK^f, F. AZAIEZ^f, TH. BYRSKI^f, D. CURIEN^f, O. DAKOV^f, G. DUCHENE^f
 F. KHALFALLAH^f, B. GALL^f, L. PIQERAS^f, J. ROBIN^f, J. DUDEK^f, N. ROWLEY^f
 N. REDON^g, F. HANNACHI^h, J.N. SCHEURER^h, J.N. WILSON^h, A. LOPEZ-MARTENSⁱ,
 A. KORICHIⁱ, K. HAUSCHILDⁱ, J. ROCCAⁱ, S. SIEMⁱ, P. FALLON^j, I.Y. LEE^j,
 A. GÖRGEN^j, A. MAJ^k, M. KMIECIK^k, M. BREKIESZ^k, J. STYCZEN^k, K. ZUBER^k,
 J.C. LISLE^l, B. CEDERWALL^m, K. LAGERGREN^m, A.O. EVANSⁿ, G. RAINOVSKIⁿ,
 G. DE ANGELIS^o, G. LA RANA^p, R. MORO^p, R.M. LIEDER^q, E.O. LIEDER^q,
 W. GAST^r, H. JÄGER^r, A.A. PASTERNAK^s, C.M. PETRACHE^t, D. PETRACHE^t

^aThe Niels Bohr Institute, University of Copenhagen, Denmark

^bISKP, University of Bonn, Germany

^cInstitute of Nuclear Research (ATOMKI), Debrecen, Hungary

^dUniversity of Debrecen, Hungary

^eDipartimento di Fisica, Università di Milano and INFN, Italy

^fIREs, IN2P3/CNRS, Strasbourg, France

^gINP, IN2P3/CNRS, Lyon, France

^hCENBG, Bordeaux-Gradignan, France

ⁱCSNSM, IN2P3/CNRS, Orsay, France

^jNuclear Science Division, LBNL, Berkeley, USA

^kInstitute of Nuclear Physics PAN, Krakow, Poland

^lBuster Laboratory, University of Manchester, UK

^mRoyal Institute of Technology, Stockholm, Sweden

ⁿOliver Lodge Laboratory, University of Liverpool, UK

^oLaboratori Nazionali di Legnaro INFN, Italy

^pDipartimento di Scienze Fisiche, Università di Napoli and INFN, Italy

^qThemba LABS, Somerset West, South Africa

^rInstitut für Kernphysik, FZ Jülich, Germany

^sIoffe Physical Technical Institute, St. Petersburg, Russia

^tDipartimento di Fisica, Università di Camerino, Italy

^uDepartamento de Física Teórica, Universidad Autónoma de Madrid, Spain

^vDepartment of Physics, University of Oslo, Norway

(Received October 2, 2006)

* Presented at the Zakopane Conference on Nuclear Physics, September 4–10, 2006, Zakopane, Poland.

The Euroball-IV γ -detector array, equipped with the ancillary charged particle detector array DIAMANT was used to study the residues of the fusion reaction ${}^{64}\text{Ni} + {}^{64}\text{Ni} \Rightarrow {}^{128}\text{Ba}$ at $E_{\text{beam}} = 255$ and 261 MeV, in an attempt to reach the highest angular momentum and verify the existence of predicted hyperdeformed rotational bands. No discrete hyperdeformed bands were identified, but nevertheless a breakthrough was obtained through a systematic search for rotational ridge structures with very large moments of inertia $J(2) \geq 100 \hbar^2 \text{MeV}^{(-1)}$, in agreement with theoretical predictions for hyperdeformed shapes. Evidence for hyperdeformation was obtained by charged particle + γ -ray gating, selecting triple correlated ridge structures in the continuum of each of the nuclei, ${}^{118}\text{Te}$, ${}^{124}\text{Xe}$ and ${}^{124,125}\text{Cs}$. In 7 additional nuclei, rotational ridges were also identified with $J(2) = 71\text{--}77\hbar^2 \text{MeV}^{(-1)}$, which most probably correspond to superdeformed shape. The angular distributions of the emitted charged particles show an excess in forward direction over expectations from pure compound evaporation, which may indicate that in-complete fusion plays an important role in the population of very elongated shapes.

PACS numbers: 21.60.-n, 21.10.Re, 27.60.+j

1. Introduction

Shortly after the discovery in 1986 of the first superdeformed (SD) discrete band in ${}^{152}\text{Dy}$ by Twin and collaborators [1], detailed predictions were made for a possible existence of hyperdeformed nuclei (HD) to appear close to the highest spin nuclei can accommodate, by Dudek and collaborators [2]. Several serious attempts were made rather early to verify these predictions, in ${}^{152}\text{Dy}$ - [3] and in the ${}^{168}\text{Yb}$ - [4] regions, but it was not possible to confirm the results for Dy [5] and the results were negative for the Yb case. During the last 5 years a new series of searches have been made, first looking for (xn) residues from the compound nuclei, ${}^{168,169,170}\text{Hf}$, ${}^{140}\text{Nd}$, ${}^{128}\text{Ba}$, ${}^{130}\text{Xe}$, and ${}^{116}\text{Sn}$, produced at the highest possible spin by symmetric or semi-symmetric fusion reactions [6]. As of today, no discrete rotational bands with large enough quadrupole moment or moment of inertia to qualify as HD has been found. However, sensitive studies of quasi-continuum states, by the so-called Rotational Plane Mapping (RPM) technique have revealed weak but distinct rotational patterns, verifying that both ${}^{126}\text{Ba}$ and ${}^{126}\text{Xe}$ have many rotational bands with large and constant moment of inertia, $J^{(2)} \approx 76$ and $83 \hbar^2 \text{MeV}^{(-1)}$, over 6–10 high spin transitions [7,8]. However, new refined theoretical calculations for this region [11,12] show that the hyperdeformed structures should be expected to have $J^{(2)} \geq 100 \hbar^2 \text{MeV}^{-1}$, indicating that the ridges found in ${}^{126}\text{Ba}$ and ${}^{126}\text{Xe}$ may instead correspond to SD bands.

As will be discussed in the following, several nuclei, ^{118}Te , $^{124,125}\text{Cs}$ and ^{124}Xe populated via light charged particle emission during the reaction have now been identified with $J^{(2)} \geq 100 \hbar^2 \text{MeV}^{-1}$ for rotational bands of 6–10 transitions. They give the first evidence for the existence of a multitude of rotational bands with hyperdeformed shape in the $A \approx 120\text{--}130$ region.

2. Theoretical expectations

A new and comprehensive discussion of the theoretical predictions and background is given in reference [12], and we discuss here only the results which are most relevant for understanding the present experimental observations. It seems rather clear today, that population of the highest spin at formation temperature, as well as the selectivity to weak rotational patterns of γ transitions are most essential for a successful experiment of this kind. At the temperature of compound formation the shell effects are mostly washed out and the nuclei are best described by liquid drop models. At the very high spins in question here the liquid drop potential passes through the Jacobi shape transition region and shows very stable potential energy surfaces especially in the $A \approx 130$ region as illustrated in Fig. 1. for the actual compound nucleus, ^{128}Ba calculated by the Lublin–Strasbourg Drop model (LSD), [10]. This model forms the basis for the shell model calculations extended to include the important region of higher temperatures in a complete macro–microscopic approach by Schunck *et al.* [12].

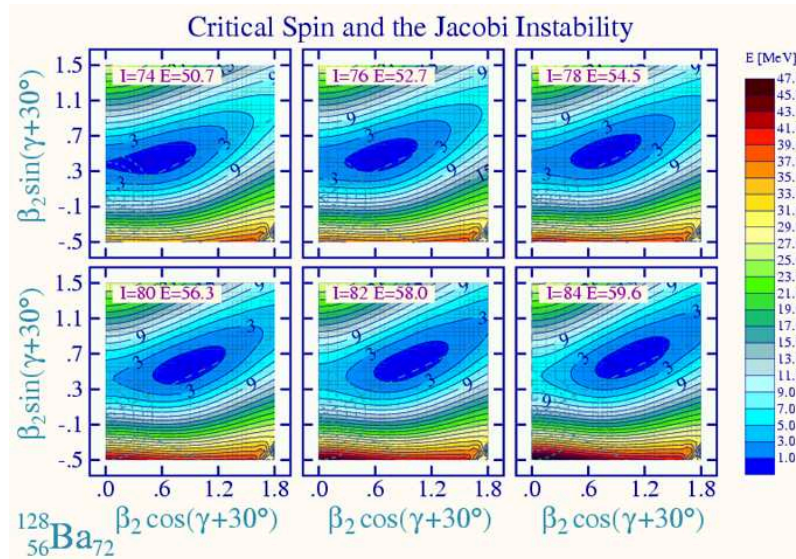


Fig. 1. Liquid drop calculation by the LSD model [10] for ^{128}Ba , showing the very stable potential energy surface at large β_2 minimum in the spin window of interest, $I = 74\text{--}84$.

Typical examples of potential energy functions along the prolate axis are shown in Fig. 2. At the high temperature and spin the nucleus will mainly be formed into elongated shapes close to hyperdeformation below a fission barrier of ≈ 7 MeV (see horizontal dashed lines). This gives a good chance of populating hyperdeformed states in the quasi-continuum at $T = 0.5$ MeV, where the shell effects clearly have stronger influence on the structure of the potential energies, resulting in 3 distinct minima for ND, SD and HD shapes. Since the moment of inertia $J^{(2)}$ of rotational bands in the 3 minima are expected to be quite different, ND ≈ 50 -, SD ≈ 80 -, HD $\approx 110 \hbar^2 \text{MeV}^{-1}$, it should be possible to recognize the rotational patterns of such bands in a study of the quasi-continuum, as will be shown below.

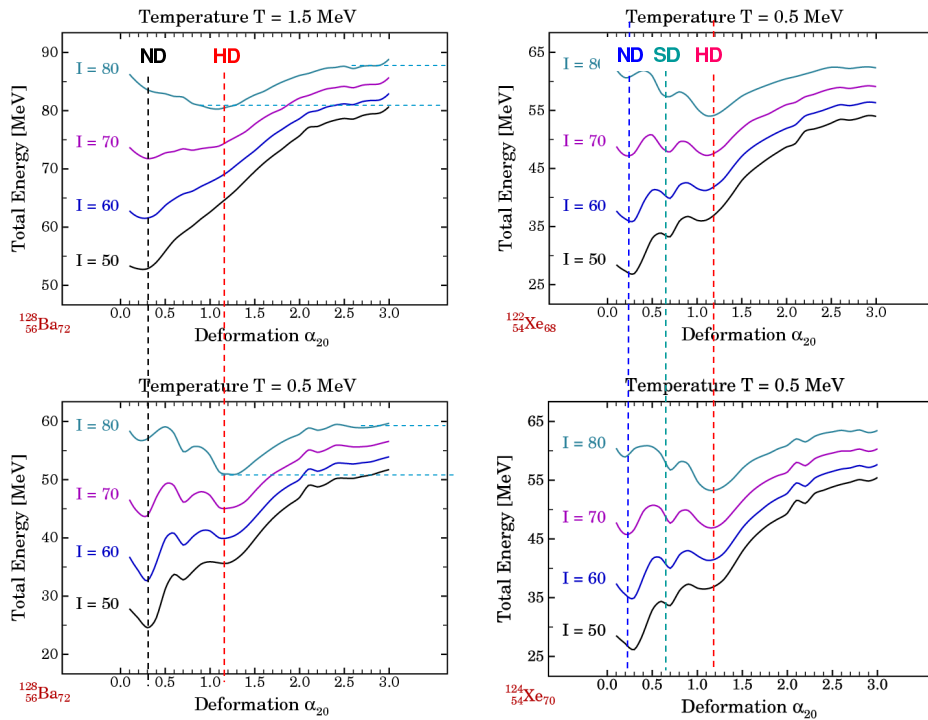


Fig. 2. Macro-microscopic calculations [12] for different spin and temperatures along the prolate axis. The vertical dashed lines indicate the stable position of the normal (ND), superdeformed (SD) and hyperdeformed (HD) minima. To the left, the potentials are shown for the compound nucleus ^{128}Ba at 2 temperatures, for ($T = 1.5$ MeV) close to the formation point and for ($T = 0.5$ MeV) close to the yrast line with shell effects more dominating. To the right, 2 of the residues discussed below are shown for the ($T = 0.5$ MeV) region where a significant part of the quasi-continuum γ -decay takes place. A net increase of the fission barrier of 2 MeV at the lower temperature is observed.

3. The experimental observations

The first observation of a ridge structure with a large moment of inertia, $J^{(2)} = 76 \hbar^2 \text{ MeV}^{-1}$ in ^{126}Ba , was made with Gammasphere (GS) at the 88" Cyclotron in LBNL, Berkeley, USA, in 2001 using the reaction $^{64}\text{Ni} + ^{64}\text{Ni} \Rightarrow ^{128}\text{Ba} \Rightarrow ^{126}\text{Ba} + 2n$ with a beam energy of 265 MeV on a target of 0.5 mg/cm^2 [7]. The necessary selectivity for the weak structures in the 2 % ($2n$) channel was obtained by applying a filter technique [13] for ^{126}Ba and adapting the Rotational Plane Mapping (RPM) technique [14,15]. Two-dimensional (2D) spectra $M_n(E_x, E_y)$ were extracted from a 3D-cube (E_x, E_z, E_y) , applying the equation:

$$M_n(E_x, E_y) : E_x + N E_y - (N + 1) E_z \in [-\delta, \delta], \quad (1)$$

where $[-\delta, \delta]$ express the thickness of the plane, defining the limits to variations in the dynamical moment of inertia for the selected rotational cascades. In addition, the uncorrelated background is removed by the so-called COR-treatment [16]. The RPM spectrum of this first experiment on ^{126}Ba is shown in Fig. 5 of Ref. [8].

The same reaction was later used in the so-called Hyper-Long-Hyper-Deformed (HLHD) experiment at the Vivitron accelerator in Strasbourg, equipped with Euroball, Inner-BGO-Ball and light-charged-particle-ball DIAMANT. The bombarding energy for the ^{64}Ni ions was changed to 255- and 261 MeV to obtain higher ($2n$) cross section, and the running time divided into 2×2 weeks. The selectivity for the $2n$ channel was further improved by applying a veto from the DIAMANT detectors when a charged particle was detected. Indeed, the ridge structure first observed at GS was clearly seen in the 261 MeV run, but it essentially vanished at a bombarding energy of 255 MeV. In fact the best spectra were obtained by a simple subtraction of raw RPM-spectra for the 255 MeV run from the corresponding RPM-spectra for the 261 MeV run, and the moment of inertia, $J^{(2)} = 76 \hbar^2 \text{ MeV}^{-1}$ was thereby confirmed. These results show that the ridge structures originate from a very narrow energy and angular momentum window, such that only the half of the 0.5 mg/cm^2 target thickness, facing the beam, was active in producing the nuclei with elongated shapes. By use of the grazing model of Winther [17], which include the collective degrees of freedom in the fusion process, and is known to reproduce the L_{max} very well, we can estimate the FWHM angular momentum window between the 255- and 261 MeV reactions to be $L_{\text{window}} \approx 78\text{--}86 \hbar$, needed to populate the ridge structures. Typical RPM-spectra for the ($2n$) reaction channel showing the HD/SD ridge is shown in Fig. 7 of Ref. [8].

A real break through in this study was recently made when a presorted database including the charged particle information became available, which gave access to many residues with further improved selectivity. RPM-spectra

gated by protons and/or α 's *i.e.* (p) , $(2p)$, (α) , (2α) and (α, p) , in addition to gating on 4–6 of the lowest γ -transitions in each of the nine strongest populated nuclei were analyzed as function of (fold + higher folds) selected by the (Inner-BGO-Ball + Ge detector shell). Since the emission of charged particles would perturb the motion of the residues, a further refinement of the Doppler correction to the gamma-spectra had to be done. Examples are shown for the most intense channels, $(\alpha 2n) \Rightarrow {}^{122}\text{Xe}$ and $(p2n) \Rightarrow {}^{125}\text{Cs}$ in Fig. 3.

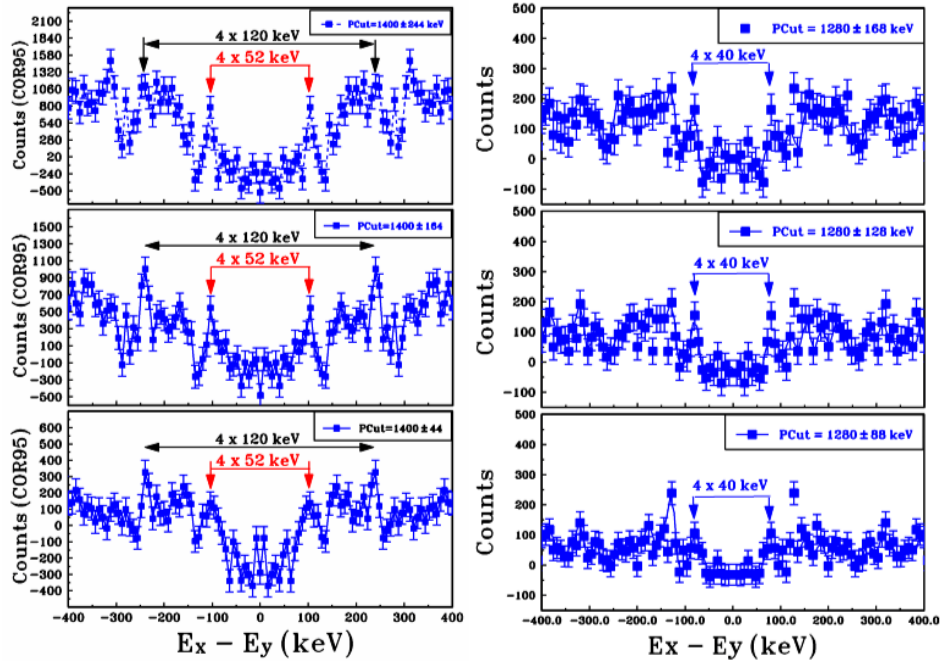


Fig. 3. Typical RPM-spectra made by PCuts across the diagonal valley, $E_{\gamma x} = E_{\gamma y}$, of Rotational Planes. The left panels show PCuts = 1440 keV with 3 different cutting widths, 88, 228, 488 keV for $(\alpha 2n) \Rightarrow {}^{122}\text{Xe}$, and the right panels show PCuts = 1280 keV with 3 different cutting width, 168, 248, 328 keV for the $(p2n) \Rightarrow {}^{125}\text{Cs}$. The marked differences between symmetric peaks in the rotational plane correspond to 2×2 decay steps of ΔE_{γ} in the rotational cascades.

The dynamical moment of inertia can be determined from the energy space between the ridges $w = 4 \Delta E_{\gamma} = 16/J^{(2)}$, and here found to be $J^{(2)} = 77$ and $100 \hbar^2 \text{MeV}^{-1}$ for the ${}^{122}\text{Xe}$ and ${}^{125}\text{Cs}$ nuclei, respectively. The perpendicular cuts (PCuts) across the diagonal valley, $E_x = E_y$, of Rotational Planes, show that the intensity of the ridges increase as expected for wider cuts. This is important, and shows that the ridges really consist of a multitude of peaks. Usually a fluctuation analysis is used to verify this, but

in the present cases statistics is marginal. We have therefore developed another statistical test, the so-called Number of Positive Channels (NPC) of the ridge structure. A smooth fit spectrum $S(E_x, E_y)$ is carefully created from the 2D rotational plane spectrum, $M(E_x, E_y)$, as in the fluctuation procedures [18], and a new NPC spectrum is made by assigning the value 1 to channels with $(M - S) > 0$ and 0 for $(M - S) \leq 0$. PCuts are then made in the same way as for RPM spectra. The NPC (height-mean) at the ridge position divided by the σ of all the fluctuations, give then an expression for goodness, like often applied to weak discrete peaks. An example of such a spectrum is shown in Fig. 4. A goodness larger than 3σ , indicate a 99 % confidence level.

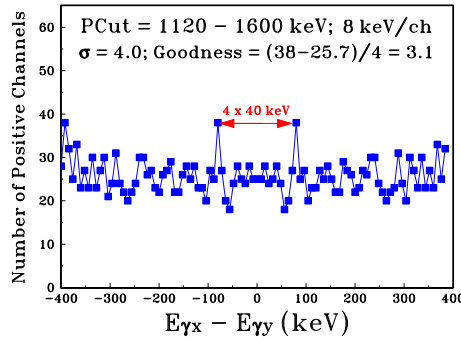


Fig. 4. NPC-spectrum (see text) for the hyperdeformed ridge structure for the $(p2n) \Rightarrow {}^{125}\text{Cs}$ channel. The goodness of peak are determined to be ≈ 3 .

Similar analysis has been made on many of the other residues, when the statistics are sufficient. In the cases when 2 charged particles are used for gating, the intensity becomes approximately 10 times weaker. However, because of the higher selectivity obtained this way even 10 times weaker structures becomes visible. Examples are shown for the $(2p2n) \Rightarrow {}^{124}\text{Xe}$ in Fig. 5.

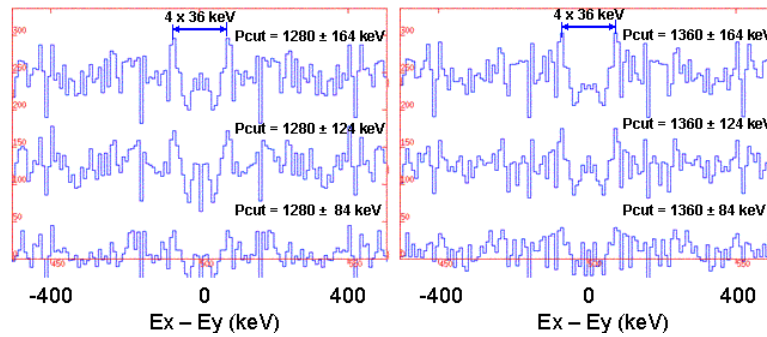


Fig. 5. RPM spectra with PCuts= 1280 ± 84 , 124 and 164 keV (left) and PCuts= 1360 ± 84 , 124 and 164 keV (right) for the $(2p2n) \Rightarrow {}^{124}\text{Xe}$.

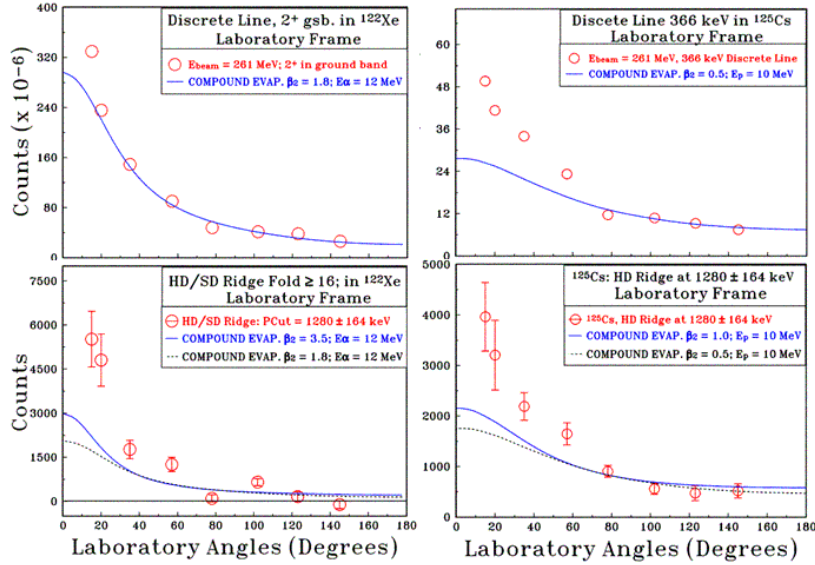


Fig. 6. Angular distributions for α -particles in coincidence with the 2^+ γ -transition in the ground state band (upper left panel), and with the SD/HD ridge structure (lower left panel) in of $(\alpha 2n) \Rightarrow {}^{122}\text{Xe}$. Angular distributions for protons in coincidence with the 366 keV γ -transition in the ground state band (upper right panel), and with the HD ridge structure (lower left panel) in $(p 2n) \Rightarrow {}^{125}\text{Cs}$.

Ridge structures are found in most cases, pointing to moment of inertias in the range $J^{(2)} \approx 70\text{--}115 \hbar^2 \text{MeV}^{-1}$. More examples of spectra are shown in Fig. 6 of Ref. [9]. A summary of the results up to now are given and compared to theoretical values for HD nuclei, in Table I.

The most narrow ridge structures are observed when the Doppler shift correction correspond to $v/c = 0.042690$, slightly smaller than expected for the full relativistic Doppler shifts, with $v/c = 0.04330$. One of the explanations considered could be that the ridges are produced via an incomplete fusion process where the α particle is emitted before the final fusion of ${}^{60}\text{Fe} + {}^{64}\text{Ni}$ takes place.

3.1. Angular distribution of the charged particles

It seems hard to understand that the ridge structure at the very highest spin can be observed both in $(2n)$ and in $(2p2n)$, $(p\alpha 2n)$ and $(2\alpha 2n)$ channels after normal compound formation and evaporation. We have, therefore, used the DIAMANT particle array to investigate if angular distributions of the charged particles used for gating, do correspond to the expectations for compound evaporation for rapidly rotating nuclei or not. The CsI detectors in DIAMANT are placed in positions corresponding to rings around

TABLE I

A preliminary summary of the results from the ridge analysis on residues from the decay of the compound nucleus ^{128}Ba .

Particle gate	γ -gate	Nucleus	ΔE_γ (keV)	$J_{\text{exp}}^{(2)}$	$J_{\text{theory}}^{(2)}$	Probable shape
xn	$(2n)$	^{126}Ba	52	77	118	SD
α	(αn)	^{123}Xe	56	71		SD
α	$(\alpha 2n)$	^{122}Xe	52	77	108	SD
α	$(\alpha 3n)$	^{121}Xe	64	63		SD
2α	(2α)	^{120}Te	56	71		SD
2α	$(2\alpha 2n)$	^{118}Te	36	111	97	HD
p	$(p 2n)$	^{125}Cs	40	100	106	HD
p	$(p 3n)$	^{124}Cs	36	111		HD
$2p$	$(2p 2n)$	^{124}Xe	36	111	111	HD
$\alpha + p$	(αpn)	^{122}I	56	71		SD
$\alpha + p$	$(\alpha p 2n)$	^{121}I	52	77	102	SD

the beam axis at $\approx 15, 20, 35, 57, 78, 102, 123$ and 145 degrees. We can determine the particle angle for each event collected in coincidence with well defined γ -ray energies, and ridge patterns. Angular distributions of evaporated particles has been treated semi-classically by Catchen *et al.* [19]. The distributions depend on spin, moment of inertia, and temperature expressed in the parameter β_2 , which we estimate to be ≈ 0.5 and 1.0 for protons emitted from intermediate or highest spin, respectively. The corresponding β_2 values for α particles are 1.8 and 3.5 .

Angular distributions for α -particles in coincidence with the $(2^+ - 0^+)$ transition and the SD/HD ridge structure in ^{122}Xe are shown in the left panels of Fig. 6, as open circles and compared to the function calculated for compound evaporation. Similar results are shown in the right panels of Fig. 6 for protons feeding the low-lying 366 keV transition, and the HD ridge structure in ^{125}Cs . For the symmetric reaction, the angular distribution in the center of mass frame will have a forward-backward symmetry, and the forward focusing of the theoretical cross section displayed in Fig. 6 is caused by the solid angle transformation to the laboratory frame. There is clearly an excess of counts at forward angles as compared to compound evaporation. This may show that a significant part of the reactions goes via an incomplete fusion process, where the light particles are emitted prior to fusion with a velocity equal to the projectile velocity, corresponding to 4 MeV for α and 1 MeV for protons. Such particles may follow Coulomb trajectories when they are emitted from the process. If this is the case they will be around $\approx 30^\circ$ and 45° in the center of mass system, corresponding to $\approx 20^\circ$ and 30°

in the laboratory system, with energies of ≈ 12 MeV and 5 MeV, respectively. It may be noted that the largest effect are seen for protons in the $(p2n) \Rightarrow {}^{124}\text{Xe}$ channel which shows HD ridge structures. Further investigations of these problems are in progress. A preliminary analysis initiated by Pasternak, was included in the presentation.

This work was supported by the Danish Science Foundation, by BMBF Germany (06BN100) and by the Polish Ministry of Science and High Education (Grant 1-P03B-030-30). The authors are grateful to the staff of the Vivitron accelerator, Strasbourg, for providing a high quality ${}^{64}\text{Ni}$ beam, smoothly over a full month of running the experiment.

REFERENCES

- [1] P.J. Twin, B.M. Nyakó, A.H. Nielson, J. Simpson, M.A. Bentley, H.W. Cranmer-Gordon, P.D. Forsyth, D. Howe, A.R. Mokhtar, J.D. Morrison, J.F. Sharpey-Shafer, G. Sletten, *Phys. Rev. Lett.* **57**, 8121 (1986).
- [2] J. Dudek, T. Werner, L.L. Riedinger, *Phys. Lett.* **B211**, 252 (1988).
- [3] A. Galindo-Uribarri, H.R. Andrews, G.C. Ball, E.E. Drake, V.P. Janszen, J.A. Kuehner, S.M. Mullins, L. Persson, D Prévost, D.C. Radford, J.C. Waddington, D. Ward, R. Wyss, *Phys. Rev. Lett.* **71**, 231 (1993).
- [4] J.N. Wilson *et al.*, *Phys. Rev.* **C56**, 2502 (1997).
- [5] M. Lunardon, N.H. Medina, G. Vesti, D. Bazzacco, D. Fabris, S. Lunardi, G. Nebbia, C. Rosso Alvarez, G. de Angelis, M. Cinausero, D. De Acuna, M. De Poli, E. Farnea, E. Fioretto, G. Prete, G. Maron, D.R. Napoli, *Phys. Rev.* **C56**, 25 (1997)7.
- [6] H. Hübel, *Acta Phys. Pol. B* **36**, 1015 (2005).
- [7] B. Herskind *et al.*, *Acta Phys. Pol. B* **34**, 2467 (2003).
- [8] B. Herskind *et al.*, *AIP Conf. Proc.* **701**, 303 (2004).
- [9] B. Herskind *et al.*, *Phys. Scr.* **T125**, 108 (2006).
- [10] K. Pomorski, J. Dudek, *Phys. Rev.* **C67**, 044316 (2003).
- [11] N. Schunck, J. Dudek, B. Herskind, *Phys. Scr.* **T125**, 218 (2006).
- [12] N. Schunck, J. Dudek, B. Herskind, *Phys. Rev.* **C** in press.
- [13] J.N. Wilson, B. Herskind, *Nucl. Instrum. Methods* **A455**, 612 (2000).
- [14] B. Herskind *et al.*, *Phys. Lett.* **B276**, 4 (1992).
- [15] S. Leoni *et al.*, *Eur. Phys. J.* **A4**, 229 (1999).
- [16] O. Andersen, J.D. Garrett, G.B. Hagemann, B. Herskind, D.L. Hillis, L.L. Riedinger, *Phys. Rev. Lett.* **43**, 687 (1979).
- [17] Aa. Winther, *Nucl. Phys.* **A594**, 203 (1995).
- [18] T. Døssing, B. Herskind, S. Leoni, A. Bracco, R.A. Broglia, M. Matsuo, E. Vigezzi, *Phys. Rep.* **268**, 1 (1996).
- [19] G.L. Catchen, M. Kaplan, J.M. Aleksander, M.F. Rivet, *Phys. Rev.* **C21**, 940 (1980).